

STRUCTURAL–FUNCTIONAL ANALYSIS OF BIOPOLYMERS AND THEIR COMPLEXES

UDC 577.2:577.32

S-DNA, Over-supercoiled DNA with a 1.94- to 2.19-Å Rise per Base Pair

L. A. Limanskaya¹ and A. P. Limansky^{1,2}

¹*Institute of Microbiology and Immunology, Academy of Medical Sciences of Ukraine,
Kharkov, 61057 Ukraine; e-mail: o.limunskyi@mail.ru*

²*Laboratory of Plasma Membrane and Nuclear Signaling, Graduate School of Biostudies,
Kyoto University, Kyoto, 606-8502 Japan*

Received May 13, 2005

Abstract—Supercoiled 3993-bp pGEMEX DNA immobilized on four substrates (freshly cleaved mica, standard amino mica, and modified amino mica with an increased or decreased surface charge density in comparison to standard amino mica) has been visualized by atomic force microscopy in the air. Plectonomically supercoiled DNA molecules, as well as single molecules with an extremely high compaction level (i.e., with a significantly higher superhelix density compared to those previously observed experimentally or estimated theoretically), have been visualized on modified amino mica with an increased surface charge density. The distance between nucleotide pairs along the duplex axis has been determined by measuring the contour length of individual oversupercoiled DNA molecules. The estimated rise per base pair varies from 1.94 to 2.19 Å. These supercoiled DNA molecules, which are compressed like a spring and have a decreased rise per base pair compared to previously known DNA forms are considered to be a new form of DNA, S-DNA. A model of S-DNA has been constructed. Molecules of S-DNA may be an intermediate in the course of the compaction of single supercoiled DNA molecules into spheroids and minitoroids. The DNA oversupercoiling, followed by the compression of the supercoiled molecules, has been shown to be accounted for by a high surface charge density of amino mica on which DNA molecules are immobilized.

DOI: 10.1134/S0026893306010158

Key words: supercoiled DNA, atomic force microscopy, AFM, amino mica, S-DNA, oversupercoiling

INTRODUCTION

The structural and physicochemical parameters of various families and forms of DNA molecules (A-, B-, C-, D-, Z-, and H-DNAs) are generally known and reliable data obtained by physical, biophysical, biochemical, and molecular genetic methods [1–3]. The conformation of the ribose ring (C'_3 -endo and C'_2 -endo in A- and B-DNAs, respectively) and the distance between base pairs along the duplex axis are among the main criteria for differentiating between the most widespread and well-known A- and B-DNA families. It is generally believed that the distance between base pairs along the axis of the DNA double helix depends on many factors (humidity, ionic conditions, etc.) and varies from 0.34–0.30 nm for B-DNA to 0.33–0.25 nm for A-DNA [2].

On the other hand, it is known that the DNA molecule is elastic and extendable like a spring. Such extended DNA molecules with an increased distance between base pairs along the duplex axis have been obtained and studied. Modern methods of micromanipulation with single molecules have been used to determine that a DNA molecule can be extended to 1.7 times its original length, with the distance

between nucleotides increasing, in the case of B-DNA, from $H = 3.4$ Å to $H = 5.8$ Å [4, 5]. The optical tweezers method was used to study the dependence of the rate of DNA replication catalyzed by DNA polymerase on the tension force applied to the DNA template. It was found that the force applied considerably affected the replication rate, which increased if the force was small and decreased if the force was greater than 4 pN. If the force was more than 20 pN, replication stopped altogether [4].

In addition to single- and double-stranded DNAs, structures of a higher order were studied. In the case of a single chromatin strand (nucleosome), the rate of the assemblage of a nucleoprotein structure (a DNA molecule wrapped around a histone octamer) considerably depended on the force applied. If the force exceeded 10 pN, the assemblage ceased, which was followed by a drastic increase in the length of the chromatin strand. However, this process was reversible: the nucleosome assemblage was resumed if the applied force decreased [6, 7].

As the DNA molecule is so elastic, one wonders whether it can be compressed like a spring. The results of studying DNA–protein complexes with the use of

atomic force microscopy (AFM) demonstrated that the contour length of DNA molecules in the absence of proteins, measured directly in AFM images, was always smaller than the theoretically expected value characteristic of B-DNA (corresponding to the distance between base pairs along the helix $H = 3.4 \text{ \AA}$). This effect was attributed to the presence of the stage of drying the sample in the course of DNA immobilization on mica, the resolution of the atomic force microscope, as well as the error of the algorithm for measuring the DNA contour length [8]. However, we believe that the mica surface characteristics (namely, the surface charge density that, in turn, determines the hydrophobic properties of the substrate) make the main contribution to the change in the conformation of DNA adsorbed on mica. Earlier studies on measuring the contour length of DNA in AFM images demonstrated that immobilization of linear DNA on the surface of freshly cleaved mica (characterized by a relatively low surface charge density) was accompanied by a partial B- to A-form transition [9]. It should also be taken into account that the aforementioned method of DNA immobilization on mica surface in a buffer solution containing Mg^{2+} ions has substantial limitations. Like other methods of DNA immobilization on mica with the use of polycations (polylysine, spermine, and spermidine), this method allows DNA to be studied in a narrow range of ionic strength ($10 \text{ mM Na}^+ < I < 200 \text{ mM Na}^+$) and, hence, a low degree of the shielding of DNA phosphate groups.

Other methods have been developed as alternative to DNA immobilization from buffer solution containing Mg^{2+} . They are based on coating mica with silicane in a vapor of an amino silane derivative [10, 11] or an aqueous solution of amino silatrane [12]. The main characteristic of amino mica so prepared is the possibility of measurements in wide ranges of pH and ionic strength. In addition, this amino mica has a higher surface charge density than freshly cleaved (unmodified) mica has [13]; however, the adhesion force characterizing the surface properties of amino mica remains the same, only slightly varying depending on the technique of substrate preparation.

Having modified the procedure of amino mica preparation in a vapor of the amino silane derivative, we developed a method for obtaining amino mica with a controlled surface charge density. This allowed us to obtain amino micas with both an increased density of surface charge (i.e., charged protonated amino groups), compared to standard amino mica [10, 11], and a decreased surface charge density.

In this study, we compared the effects of surface properties of four substrates for AFM visualization of DNA (freshly cleaved mica, standard amino mica, and amino micas with an increased and decreased surface charge densities) on the conformation of both helical and linear DNA molecules. The use of modified amino

mica with an increased surface charge density and hydrophobicity allowed us to visualize different stages of oversupercoiling of circular DNAs resulting in the appearance of a supercoil axis of molecules of the second and third orders, as well as the compaction of single supercoiled DNAs into hemispheroids and spheroids. In addition to highly compact DNA molecules, we visualized single molecules of supercoiled DNA, which we assume to result from the transition between plectonically supercoiled DNAs and highly compact structures formed not only by monomers, but also by dimers and trimers. By measuring the contour lengths of supercoiled DNA molecules in AFM images, we determined the rise per base pair along the double helix axis for these supercoiled molecules. The values obtained ($H = 1.94\text{--}2.19 \text{ \AA}$) indicate that a decrease in rise per base pair along the duplex axis is one of the mechanisms of DNA compaction. We consider these supercoiled DNA molecules with a rise per base pair of $H = 1.94\text{--}2.19 \text{ \AA}$ to be a novel DNA form which we have termed S-DNA (S stands for *spring*). Indeed, elastic supercoiled DNA molecules on the mica surface resemble springs: they can be both compressed, with the rise per base pair decreased, and extended (in this study, we obtained images of stretched supercoiled DNA molecules with a rise per base pair of $H = 4.87\text{--}5.36 \text{ \AA}$).

EXPERIMENTAL

DNA preparation for AFM. We used supercoiled 3993-bp pGEMEX DNA (Promega, United States) and 1414-bp linear DNA obtained by amplifying a linearized pGEMEX DNA. Freshly cleaved mica, standard amino mica, and modified amino micas with surface amino group densities increased and decreased, compared to standard amino mica, served as substrates. To apply DNA on freshly cleaved mica, we used a 10 mM HEPES buffer solution containing 2.5 mM MgCl_2 . A 10- μl drop of a 0.1–1 $\mu\text{g/ml}$ DNA solution buffered with TE (10 mM Tris-HCl (pH 7.9) and 1 mM EDTA) was applied on a strip of amino mica or modified amino mica 1 cm^2 in size, exposed for 2 min, washed with deionized water, blown with a flow of argon, and incubated at a pressure of 100 mm Hg for 20 min. Standard mica was obtained as described in [14] by modifying freshly cleaved mica with amino groups in a vapor of distilled 3-aminopropyl triethoxysilane (APTES) and *N,N*-diisopropyl ethylamine. The reagents were from Aldrich (United States) and Wakenyaku (Japan). APTES was distilled in an atmosphere of argon at low pressure. For amine modification, freshly cleaved mica was incubated in the presence of APTES and *N,N*-diisopropyl ethylamine solutions in a 2.5-l glass desiccator filled with argon for 1 h. The modified mica was stored in the desiccator in an argon atmosphere for one month. To prepare buffer solutions and DNA samples, we used ultrapure

water with a specific electrical resistance of $\sim 17 \text{ M}\Omega \text{ cm}$ obtained with the use of a Milli Q device (Millipore, United States). Modified amino mica was obtained by slightly altering the technique for obtaining standard amino mica. Amino mica with a decreased surface amino group density was obtained via treating freshly cleaved mica with a vapor of undistilled APTES by the method similar to that used for obtaining standard amino mica.

DNA preparation for PCR. For PCR, we used linear DNA obtained by digesting supercoiled pGEMEX DNA with *ScaI* restriction endonuclease (New England Biolabs, United Kingdom). We constructed primers L1 and L2 that determined a DNA fragment containing the promoter and transcription termination region of T7 RNA polymerase. The L1 and L2 primers were obtained from Sigma (United States). Their sequences and the corresponding positions on pGEMEX DNA were as follows:

5'-cgc tta caa ttt cca ttc gcc att c-3'
forward primer L1 (3748–3772)

5'-ctg att ctg tgg ata acc gta tta ccg-3'
reverse primer L2 (1168–1142)

Hot-start PCR was performed in 50 μl of reaction mixture using a GeneAmp 9700 amplifier (Perkin Elmer, United States) at the following temperature and time parameters: initial incubation, 2 min at 95°C; denaturing, 1 min at 95°C; annealing, 1 min at 69–73°C; synthesis, 1 min at 74°C; number of cycles, 35. To perform PCR, we used two forms of thermostable high-precision DNA polymerase: Pyrobest DNA polymerase (TaKaRa, Japan) and Invitrogen Platinum DNA polymerase (Invitrogen, Japan). The reaction mixture contained 2.5 U of DNA polymerase, reaction buffer solution, 2.5 mM MgCl_2 , 0.2 mM dNTP, 1 μM of each primer, and a DNA template. The annealing temperature was determined theoretically using the Oligo software. To minimize the amplification of non-specific fragments, we performed PCR several times at different annealing temperatures (69, 71, and 73°C). To visualize the amplicons, 15 μl of the PCR product was separated by electrophoresis in 2% (by volume) TAE agarose gel and stained with ethidium bromide.

The following procedure was used to purify the amplified DNA fragment. After the completion of electrophoresis, the strip that contained the amplicon was cut from the gel with the use of a low-intensity long-wave UV light source (BioRad, United States). We subsequently purified the amplicon from nucleotides, primers, DNA polymerase, and ethidium bromide with the use of a QIAquick PCR Purification Kit (QIAGEN, Japan) as recommended by the manufacturer, extracted it with a phenol–chloroform mixture, and reprecipitated with ethanol.

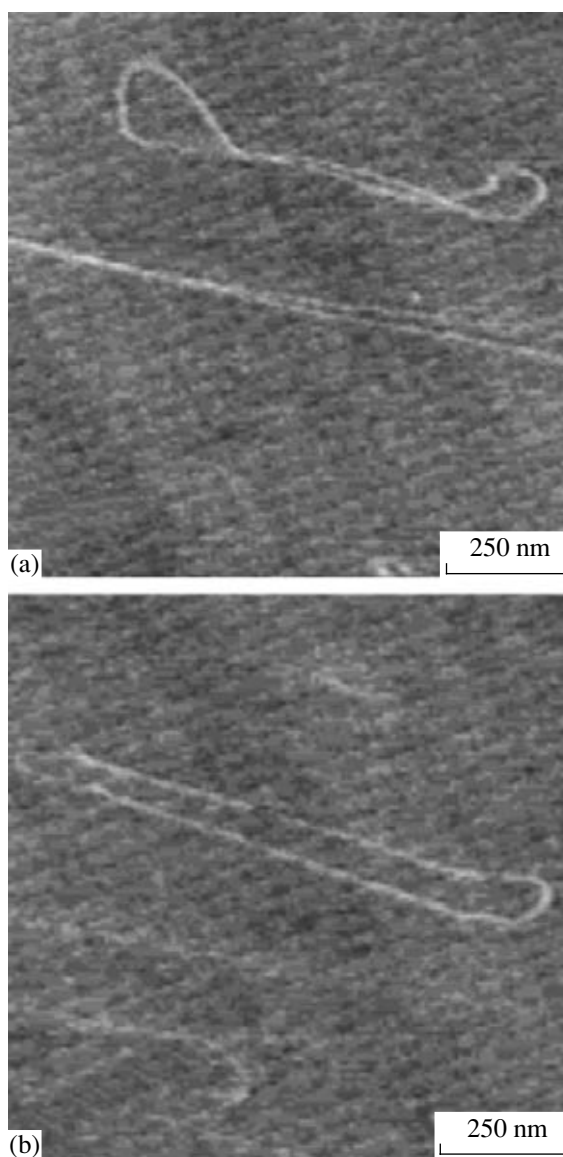


Fig. 1. AFM images of stretched supercoiled pGEMEX DNA molecules immobilized on amino mica with a decreased amino group density. (a) The DNA contour length is $L = 1943 \text{ nm}$, which corresponds to a rise per base pair along the double helix axis of $H = 4.87 \text{ \AA}$. The frame size is $1.13 \times 1.13 \mu\text{m}$. (b) The DNA contour length is $L = 2140 \text{ nm}$; $H = 5.36 \text{ \AA}$. The frame size is $1.07 \times 1.07 \mu\text{m}$.

Atomic force microscopy. We used a Nanoscope IV MultiMode System atomic force microscope (Veeco Instruments, United States) equipped with an E-scanner (with a maximum range of 12 μm). AFM images of DNA were recorded using the vibrating variant of AFM in the air in the mode *height* at room temperature. Scanning was performed by means of OMCL-AC160TS cantilevers (Olympus Optical, Japan) with a resonance frequency of 340–360 kHz and a constant rigidity of 42 N/m, at a scanning frequency of 3 Hz. The images were obtained in the

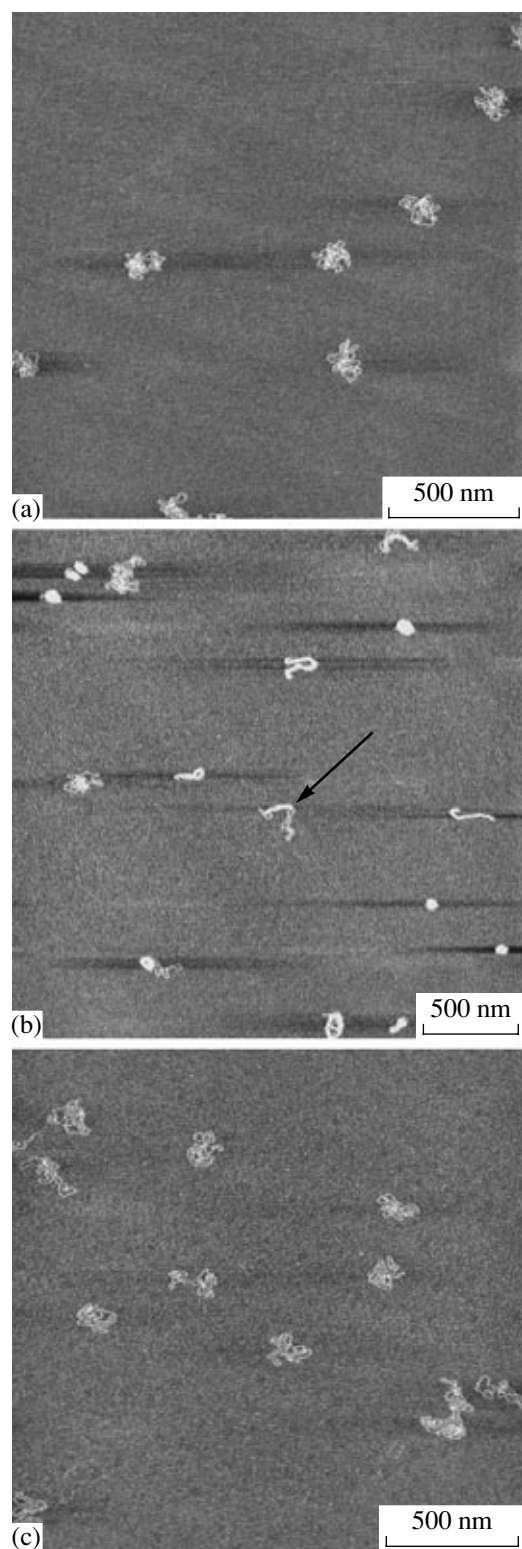


Fig. 2. AFM images of a 3993-bp supercoiled pGEMEX DNA in air obtained after DNA dissolved in a TE buffer solution was applied on the surface of (a) standard amino mica and (b) modified amino mica characterized by a higher surface amino group density (i.e., an increased charge density) compared to standard amino mica. The figure shows supercoiled DNA with different degrees of compaction, from (a, c) plectonometrically supercoiled to (b) oversupercoiled molecules with different lengths of the supercoil axis. Frame sizes: (a) $2 \times 2 \mu\text{m}$; (b) $2.7 \times 2.7 \mu\text{m}$; (c) $2 \times 2 \mu\text{m}$. (a, b) Freshly prepared mica; (c) modified mica after two weeks of storage. The arrow indicates a supercoiled DNA molecule whose AFM image at a greater resolution is shown in Fig. 3b.

512×512 pixel format, smoothed, and analyzed with the use of the Nanoscope (version 5.12r3) software, (Veeco Instruments, United States).

The volume of DNA molecules was calculated on the basis of their actual parameters measured in the AFM image (the height, length, and width of the molecules), without a correction for widening the DNA diameter. To measure the volume of molecules more accurately, we constructed longitudinal and, usually, transverse sections of the molecules with the use of a built-in option of the Nanoscope software.

RESULTS AND DISCUSSION

The surface of mica, a standard substrate for immobilizing biomolecules in AFM studies, is negatively charged in buffer solutions at neutral pH values and a low ionic strength [15]. Therefore, several methods of changing the total surface charge from negative to positive are used to absorb negatively charged DNA molecules on mica surface under the given conditions. The simplest method is to add Mg^{2+} or Ni^{2+} ions to the DNA solution a drop of which is applied on the surface of freshly cleaved mica [16]. Alternative approaches involve the modification of the mica surface with various polycations, such as polylysine, spermine, and spermidine [17–19]. However, all of these approaches have one substantial drawback: DNA can be immobilized on mica in very narrow ranges of pH and ionic strength, which makes it impossible to markedly change the surface charge density of the substrate.

We modified the method of amino modification of AFM probes in a vapor of APTES, an aminosilane derivative, that we developed earlier [20] to use it for obtaining amino mica with desirable characteristics, i.e., with a controlled surface charge density. By modifying the standard procedure for obtaining amino mica (the surface of which has a positive charge in a wide range of both pH and ionic strength of the solution), we obtained amino micas with both increased and decreased surface charge densities compared to standard amino mica. Hereinafter, by modified amino mica we mean amino mica with an increased surface charge density, unless otherwise indicated.

Figure 1 shows the AFM image of stretched supercoiled pGEMEX DNA molecules immobilized on amino mica with a decreased surface charge density [21]. Stretched DNA molecules were formed during the preparation of the specimen for AFM, when the mica

was washed with ultrapure water after exposure in the presence of DNA solution. The increase in the contour length of stretched pGEMEX DNA molecules to $L = 1943$ nm (Fig. 1a) and $L = 2140$ nm (Fig. 1b) indicates that the extension of the supercoiled DNA increases the rise per base pair from $H = 4.87$ Å and $H = 5.36$ Å, respectively. The data obtained for stretched pGEMEX DNA molecules agree with published results of studies on stretched DNAs performed by various methods [22].

The AFM images of supercoiled pGEMEX DNA shown in Fig. 2 demonstrate that the surface characteristics of amino mica substantially affected the conformation of DNA molecules. The molecules immobilized on standard amino mica (Fig. 2a) were in a conformation similar to plectonomic, whereas an increase in the surface charge density led to a striking compaction of DNA molecules (Fig. 2b). In addition to numerous highly compacted molecules, we visualized oversupercoiled DNA molecules that drastically differed in shape from both the plectonomically supercoiled DNA molecules obtained on standard amino mica (Fig. 2a) and the supercoiled molecules obtained on modified amino mica (with an increased charge density) that was stored for two weeks before DNA immobilization (Fig. 2c). One of these supercoiled DNA molecules is indicated by an arrow in Fig. 2b. The frames shown in Fig. 2 are comparatively large ($\sim 2 \times 2$ μm) and demonstrate that the surface of amino mica contained only DNA molecules; it was free of impurities, foreign nanoparticles, which are encountered in some AFM studies.

It is crucially important for estimating the surface characteristics of modified amino mica that the DNA image (the shape and number of molecules) on modified amino mica stored for two weeks before use (Fig. 2c) were similar to the AFM image of the molecules on freshly made standard amino mica (Fig. 2a). This means that, first, the number of active (protonated) amino groups on the surface of modified amino mica was considerably larger than the number of amino groups on the surface of standard amino mica (note that the results of earlier X-ray photoelectron spectroscopic studies [23] showed that only 50% of amino groups on the surface of standard amino mica were active) and, second, their resistance to oxidation is considerably higher than that of the amino groups of standard amino mica. Earlier, we found that the number of amino groups on the surface of standard amino mica considerably decreased after two weeks of stor-

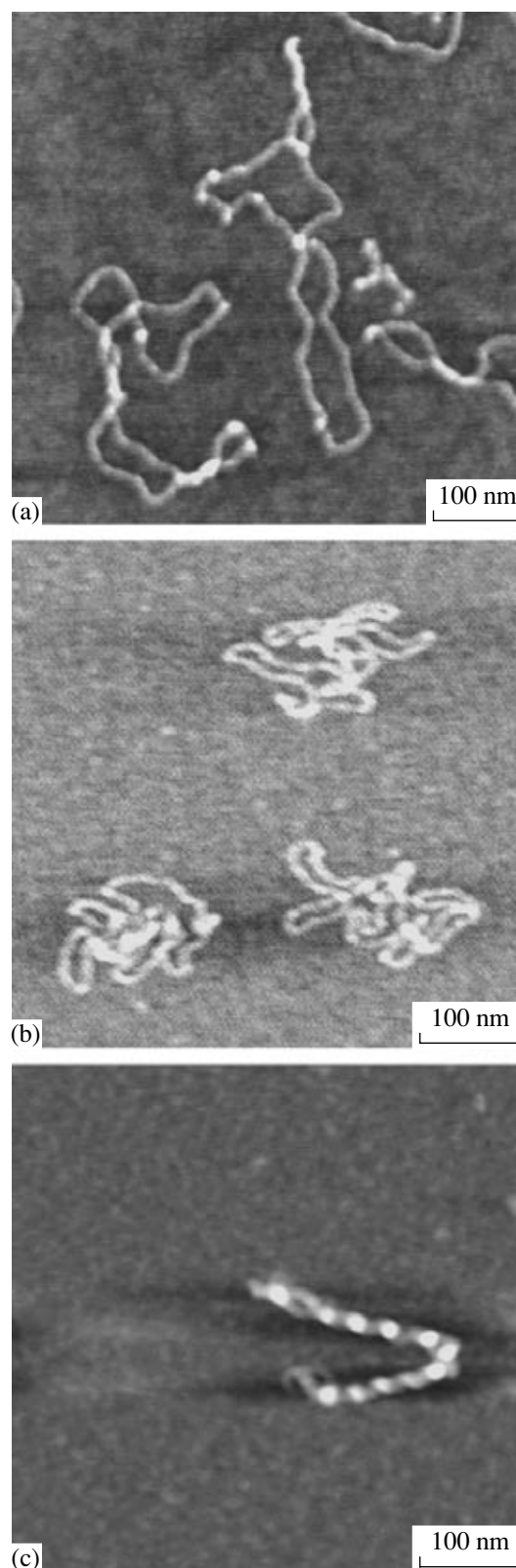


Fig. 3. AFM images of single supercoiled pGEMEX DNA molecules immobilized on (a) freshly cleaved mica (the image has been obtained after applying a drop of DNA dissolved in a 10 mM HEPES buffer solution containing 2.5 mM $MgCl_2$), (b) standard amino mica, and (c) modified amino mica. Frame sizes: (a) 583×583 nm; (b) 500×500 nm; (c) 500×500 nm. Contour lengths of the pGEMEX DNAs: (a) 1243 nm, (b) 1216 nm, and (c) 873 nm. The lengths of the supercoil axes of the DNA molecules: (a) 466 nm, (c) 382 nm.

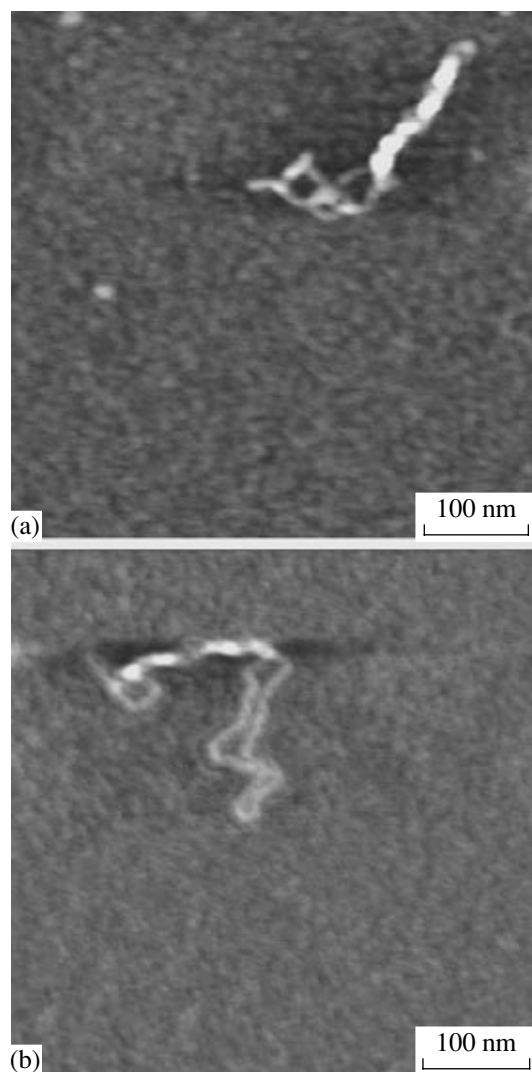


Fig. 4. AFM images of supercoiled pGEMEX DNA molecules on modified amino mica. The frame size in 500×500 nm in both images. (a) The contour length of the DNA molecule is 776 nm, which corresponds to a rise per base pair along the double helix axis of $H = 1.94$ Å. (b) The contour length of the DNA molecule is 852 nm, which corresponds to a rise per base pair along the duplex axis of $H = 2.11$ Å.

age, and the half-activity period of standard amino mica was estimated to be precisely two weeks. Thus, modified amino mica considerably surpasses standard amino mica in the stability and surface density of amino groups. Due to these differences, immobilization of supercoiled DNA on modified amino mica allowed us to obtain images of individual DNA molecules with an extremely high level of supercoiling that had not been previously observed experimentally or even considered theoretically. It is also important that the oversupercoiled DNA is considerably more sensitive to the surface characteristics of the substrate compared to linear DNA. Let us analyze these oversupercoiled DNA molecules in more detail.




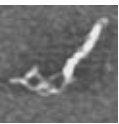
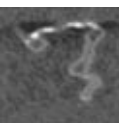
Several parameters are commonly used to characterize the topology of supercoiled DNAs (molecules whose axis may be coiled, in contrast to linear DNAs). These are supercoiling density, the number of nodes (supercoils), and the supercoil axis length. The supercoiling density (σ) may be defined as the ratio of the number of supercoils to the number of coils in a relaxed double helix [24]. Images of DNA molecules obtained at a higher resolution (Fig. 3) demonstrate striking differences in topology between DNA molecules immobilized from a buffer solution containing 2.5 mM $MgCl_2$ on freshly cleaved mica (Fig. 3a), standard amino mica (Fig. 3b), and modified amino mica (Fig. 3c). Figure 3a shows the images of plectonomically supercoiled DNA molecules characterized by a low supercoiling density (seven supercoils or nodes, $\sigma = -0.018$). Earlier, similar images were obtained for plasmid DNAs on substrates treated with the polycations polylysine and spermine [18, 19]. Supercoiled pGEMEX DNA molecules immobilized on standard amino mica (Fig. 3b) were more compact; however, their contour length measured in the AFM image was only slightly shorter ($L = 1216$ nm) than that of plectonomically supercoiled DNA on mica that had Mg^{2+} ions on its surface ($L = 1243$ nm, Fig. 3a).

The supercoiled DNA molecule immobilized on modified amino mica that is shown in Fig. 3c considerably differed from the DNA molecules shown in Figs. 3a and 3b in all its parameters: the number of nodes was increased to 11, the supercoil axis was shortened to 382 nm, and the contour length calculated from the AFM images was $L = 873$ nm (!).

The measurement of the length of a single native DNA molecule at a subnanometer resolution, which is a characteristic feature of AFM, makes it possible to determine the distance between base pairs along the axis of the DNA double helix (the rise per base pair), provided that the number of nucleotides in the given molecule is known. Whereas the rise per base pair for the pGEMEX DNA molecule shown in Fig. 3a is $H = 3.11$ Å, this value calculated for the oversupercoiled DNA shown in Fig. 3c was as small as $H = 2.19$ Å (!). The value $H = 3.11$ Å agrees with earlier data on a slight decrease in the contour length of DNA dried on mica, if the DNA is assumed to be B-DNA [8]. However, the value $H = 2.19$ Å indicates that supercoiled DNA molecules immobilized on amino mica with an increased charge density undergo considerable intramolecular changes that not only increase the degree of supercoiling, but also decrease the rise per base pair.

Figure 4 shows other AFM images of individual supercoiled pGEMEX DNA molecules on modified amino mica. The rises per base pair calculated for the oversupercoiled molecules shown in Figs. 4a and 4b, respectively, are $H = 1.94$ Å and $H = 2.11$ Å. We used the volume of a DNA molecule calculated directly

Table 1. Parameters of supercoiled pGEMEX DNA molecules determined from AFM images

No.	Molecule	Height (h_{\max} , nm)	Height (h_{\min} , nm)	Contour length of an oversupercoiled molecule (L , nm)	Length of the supercoil axis (l , nm)	Contour length of a relaxed molecule (L_{relax} , nm)	Rise per base pair (H , Å)	Volume (V , nm ³)
1 ^a		0.80	0.35*	1243	466	1243	3.11	3510
2 ^b		0.99	0.35*	1216	–	1216	3.05	3530
3		2.00	0.35*	390	370	873	2.19	3830
4		1.80	0.27*	577	282	776	1.94	3830
5		1.33	0.35*	642	390	852	2.11	3800

Note: The theoretical excluded volume of pGEMEX DNA is $V = 4010 \text{ nm}^3$.

* Double-stranded DNA; ^a DNA immobilized on mica in a buffer solution containing MgCl_2 ; ^b DNA immobilized on standard amino mica.

from its AFM image as a parameter that allowed a single molecule to be distinguished from a dimer or another highly compact structure formed by several molecules. Its value for single DNA molecules insignificantly differed from the theoretically expected excluded volume of the molecule ($V_{\text{excl}} = 4010 \text{ nm}^3$) and permitted reliable differentiation between single DNA molecules and aggregations. To calculate the volume more accurately, we usually used the longitudinal section of the molecule by a plane perpendicular to the plane of the mica, rather than the height of the molecule measured at one point (which considerably varies for oversupercoiled DNAs: given the characteristic height of one strand of the double helix $h = 0.3\text{--}0.4 \text{ nm}$, the height at nodes formed by two intersecting DNA strands may be as large as $1.3\text{--}1.8 \text{ nm}$).

As evident from the parameters of DNA molecules shown in Table 1, the volume of oversupercoiled DNA molecules (nos. 3–5 in Table 1; Figs. 3c, 4) agreed, within the experimental error, with the volume of a single supercoiled DNA molecule immobilized on either freshly cleaved mica or standard amino mica (nos. 1, 2 in Table 1; Figs. 2a, 2b). The volumes (V) of dimers (nos. 3–6 in Table 2) and trimers (no. 7 in Table 2) were, respectively, two and three times larger than the volume of a single molecule. Note that highly compact structures, hemispheroids (no. 1 in Table 2) and


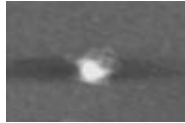
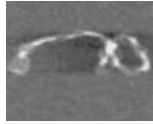

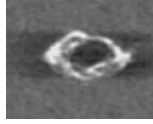
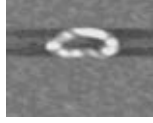

spheroids (no. 2 in Table 2), were also formed by single molecules. The substantially smaller volume of the spheroid (no. 2 in Table 2), compared to that of a single molecule, is explained by the fact that volume of DNA strands protruding from the spheroid was not taken into account.

Oversupercoiled Molecules Are Formed by Single DNA Molecules

The calculation of the volumes of condensed structures permitted unambiguous differentiation between aggregations (dimers, trimers, etc.) and single DNA molecules. To calculate the volume of the oversupercoiled DNA molecule shown in Fig. 5a, we constructed three longitudinal sections of the fragments of the molecule, two of which are shown in Figs. 5b and 5c. The resultant volume of this oversupercoiled molecule (no. 3 in Table 1) fit both the experimentally determined excluded volume of a single supercoiled DNA molecule (no. 1 in Table 1) in the AFM image and the value calculated theoretically.

The height of wound threads formed by double-stranded DNAs is another important evidence that single molecules rather than wisps are supercoiled. Arrows in the AFM image (Fig. 5a) and the three-dimensional image of this molecule indicate clearly

Table 2. Parameters of compacted structures formed by (1, 2) one, (3–6) two, and (7) three supercoiled pGEMEX DNA molecules determined from AFM images

No.	Molecules	Height (h_{\max} , nm)	Height (h_{\min} , nm)	Contour length of the oversupercoiled molecule (L , nm)	Length of the supercoil axis (l , nm)	Volume (V , nm ³)
1		2.60	1.85	–	–	3620
2		3.45	0.30*	–	–	3140
3		1.40	0.35*	548	548	6300
4		2.00	0.87	269	269	7080
5		2.00	0.45*	–	401	6840
6		2.10	0.30*	267	267	6570
7		3.50	1.00	260	260	10650

* Double-stranded DNA.

distinguishable threads. The measured height of these partly disjointed threads (Fig. 5e) showed that they were formed by double-stranded DNA, because the height of each thread ($h = 0.38$ nm) was the same as the height of a single DNA molecule immobilized on unmodified mica (no. 1 in Table 1), which, in turn, agreed with published AFM estimates of the height of

Table 3. Parameters of A-, B-, and S-DNAs

	A-DNA	B-DNA	S-DNA
Rise per base pair along the helix axis, Å	2.56–3.29	3.03–3.37	1.94–2.19
Base slope, deg	20.2–10	16.4–5.9	30.5–27
Distance between bases, Å	2.72–3.34	3.16–3.39	2.25–2.45

DNA adsorbed on a substrate [18]. Similar measurements were made for another supercoiled DNA (Fig. 6). Both the volume (no. 4 in Table 1) and the measured height of the threads of this molecule ($h = 0.38$ – 0.40 nm) confirmed that a single (!) DNA molecule formed this structure. The volumes of other visualized highly compact structures shown in Table 2, namely, the hemispheroid (no. 1), spheroid (no. 2), dimers (nos. 3–6), and the trimer (no. 7), confirm the reliability of this method for determining the volumes of condensed structures, as well as the effectiveness of their differentiation.

We consider these supercoiled DNAs, in which the rise per base pair along the duplex axis ($H \sim 2$ Å) is decreased, compared to well-known DNA forms, to be a novel form of DNA, which we have termed S-DNA (S stands for *spring*).

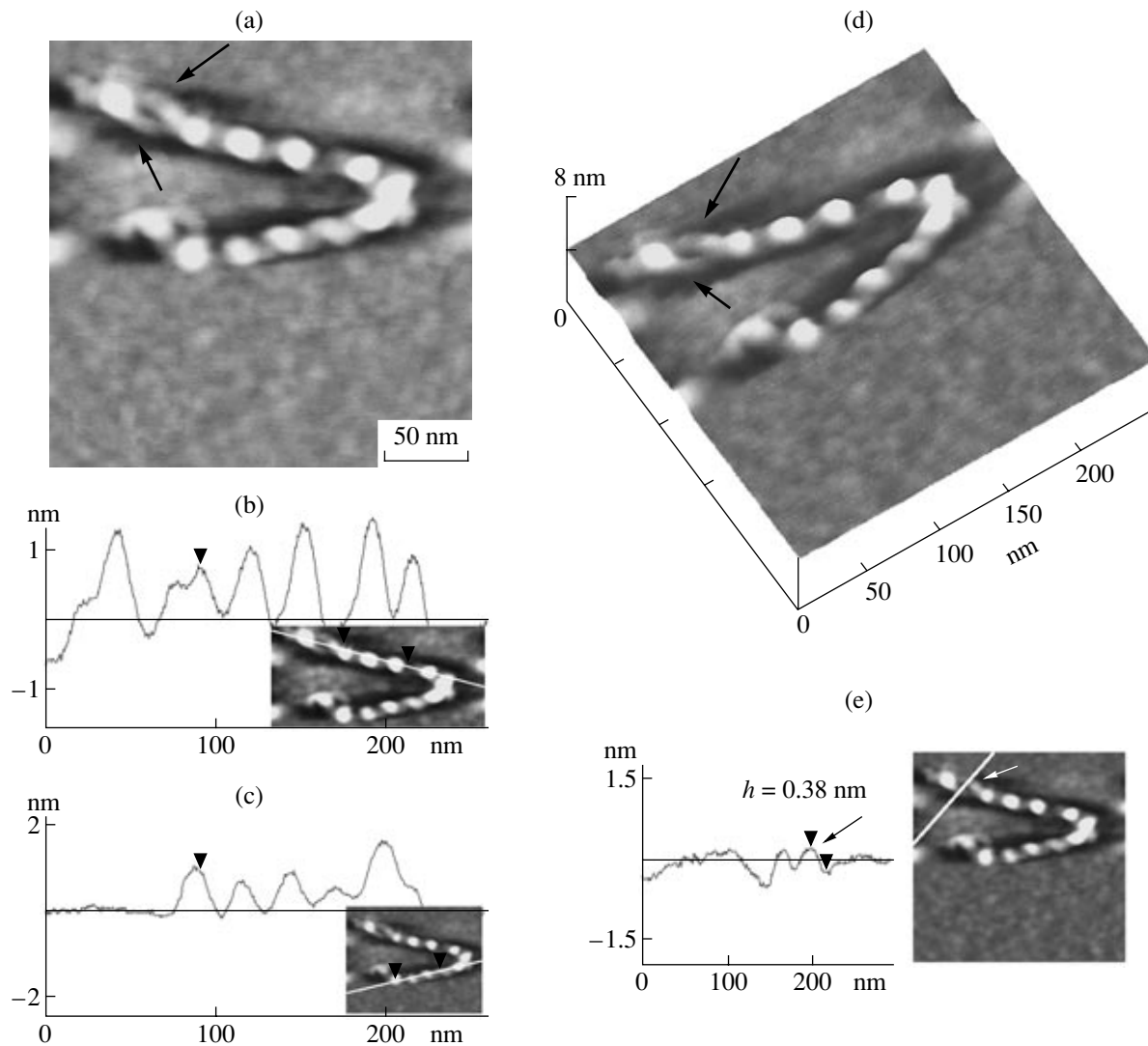


Fig. 5. (a) AFM image of a single oversupercoiled pGEMEX S-DNA obtained after the immobilization on the surface of modified amino mica characterized by a high surface charge density. The frame size is 250×250 nm. The rise per base pair along the duplex axis for this molecule is $H = 2.19$ Å. Arrows indicate two threads, each formed by a DNA double helix, twisted into a right oversupercoiled DNA with distinct 11 supercoils (nodes). (b, c) Longitudinal sections of the pGEMEX DNA molecule. The section plane is perpendicular to the plane of the figure; the line at which the two planes intersect is shown in the insets. The molecule volume has been calculated as the product of the molecule width and the sum of the cross-section areas. (b) Six or (c) five peaks in the section profiles correspond to six and five nodes, respectively. (d) The three-dimensional image of the molecule. The arrows indicate partly separated threads of the duplex forming the oversupercoiled molecule. (e) The transverse section through the separated threads of the duplex. The inset shows the line at which the section plane is drawn perpendicular to the plane of the figure. Two peaks correspond to the section profiles of the two threads that were used to determine their heights. The maximum height of the peak corresponds to the height of the molecule fragment. The arrows at the section and the inset indicate the peak and the corresponding DNA double helix with a height of $h = 0.38 \pm 0.05$ nm.

It was earlier demonstrated that the rise per base pair in a double-stranded DNA was linearly related to the slope of the bases relative to the helix axis [2]. Figure 7 shows the plot approximated to a rise per base pair of $H = 1.9$ Å. The module of the slope of bases in S-DNA (γ) determined from this plot falls within the interval $27^\circ < \gamma < 30.5^\circ$, which corresponds to the range of rise per base pair values $1.94 \text{ Å} \leq H \leq 2.19 \text{ Å}$. Although the A- to B-form transition, when the rise per base pair increases, is accompanied by a

change of the sign of γ from positive to negative, we have no data on the sign of γ in the case of the slope of bases in S-DNA.

To understand the mechanism of DNA elasticity more comprehensively, we preliminarily studied the compressibility of linear DNA molecules, taking into account that the contour length of linear DNA was earlier found to decrease upon the immobilization on mica with a low surface charge density [8]. For this

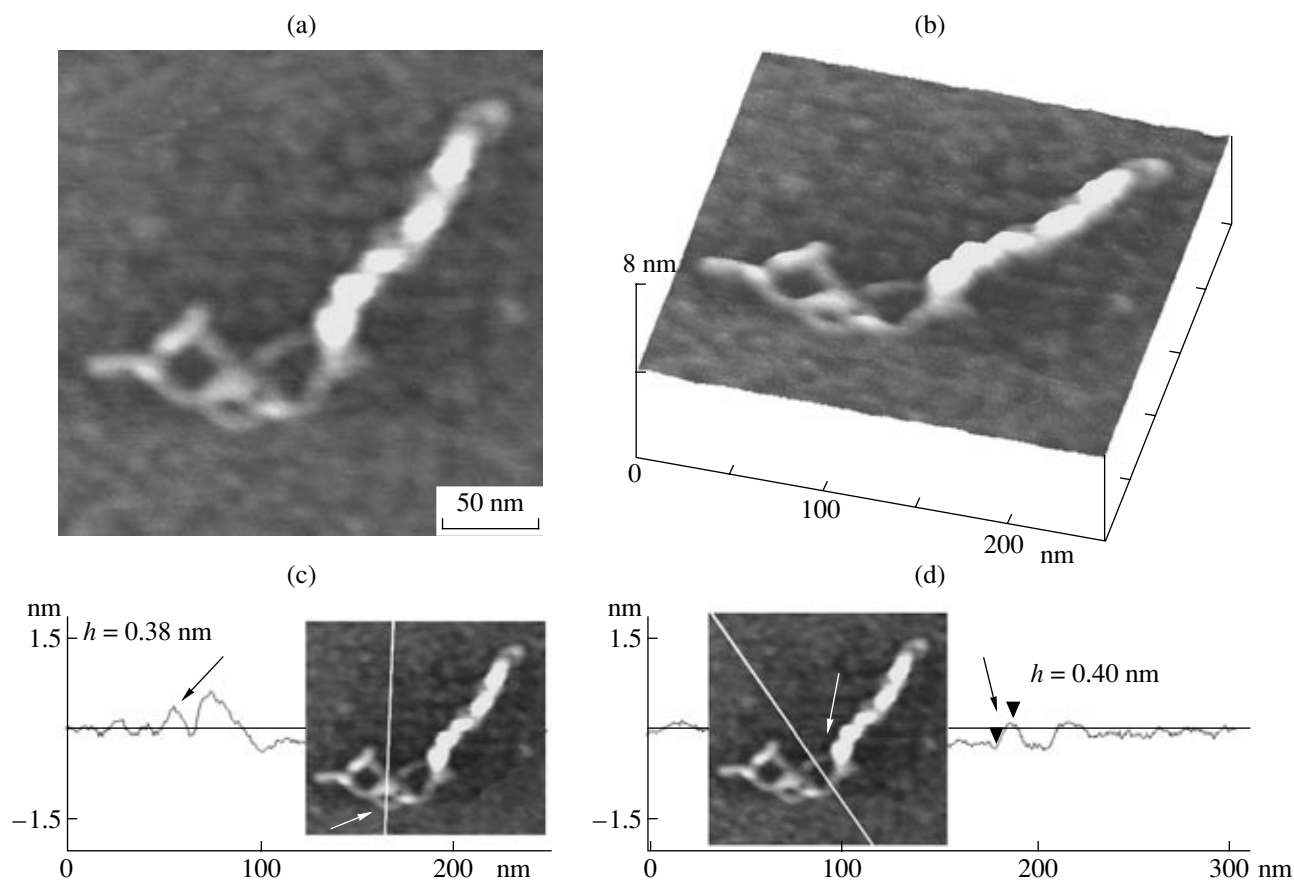


Fig. 6. (a) The AFM image of a single left oversupercoiled pGEMEX S-DNA. The frame size is 250×250 nm. (b) The three-dimensional image of the molecule. (c) The profile of the transverse section along the line shown in the inset. The arrows indicate the peak and the corresponding fragment of the thread of the DNA double helix with a height of $h = 0.38$ nm. (d) The profile of the transverse section along the line shown in the inset. The arrow indicates the peak that was used to determine the height of the corresponding part of the DNA double helix, $h = 0.40$ nm.

purpose, 1414-bp linear DNA was immobilized on freshly cleaved mica (Fig. 8a) and modified amino mica (Fig. 8b). The contour length of molecules was determined from the distributions of the contour

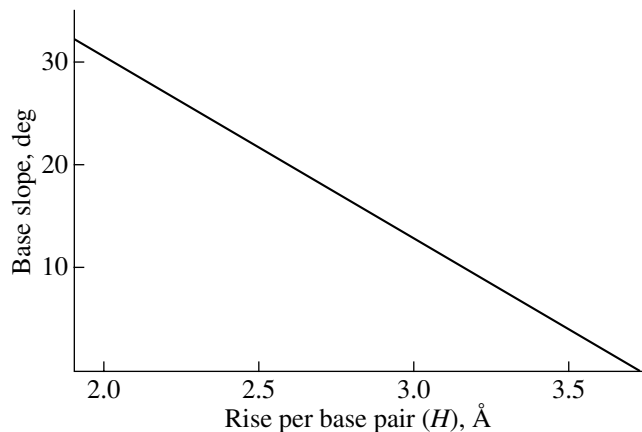


Fig. 7. Dependence of the slope of bases on the rise per base pair along the double helix axis. The base slope is defined as the angle between the perpendicular to the plane of the base and the duplex axis.

length of visualized replicons. For DNA molecules immobilized on freshly cleaved mica, the contour length was $L = 435 \pm 15$ nm (Fig. 9), which corresponded to a rise per base pair along the helix axis of $H = 3.10$ Å. This value falls within the intervals of the rise per base pair in both B-DNA (3.03 Å $< H < 3.37$ Å) and A-DNA (2.56 Å $< H < 3.29$ Å) [2]. The contour length of the amplicon immobilized on modified amino mica was $L = 296 \pm 14$ nm, which corresponded to rise per base pair along the duplex axis of $H = 2.09$ Å. Some of the numerous DNA structural parameters (the slopes of bases and the axis, rise per base pair along the duplex axis, propeller twist, coil repeat, etc.) are shown in Table 3 for the case of compressed S-DNA as compared with previously known forms, A- and B-DNAs. Note that A-DNA may be considered a compressed molecule compared to B-DNA.

Do spatial restrictions for nucleotides exist in S-DNA? Our models of a 15-bp fragment of S-DNA (Fig. 10a) and B-DNA (Fig. 10b) demonstrate that, in principle, there may be compressed DNA molecules with a rise per base pair along the duplex axis decreased to $H \sim 2$ Å.

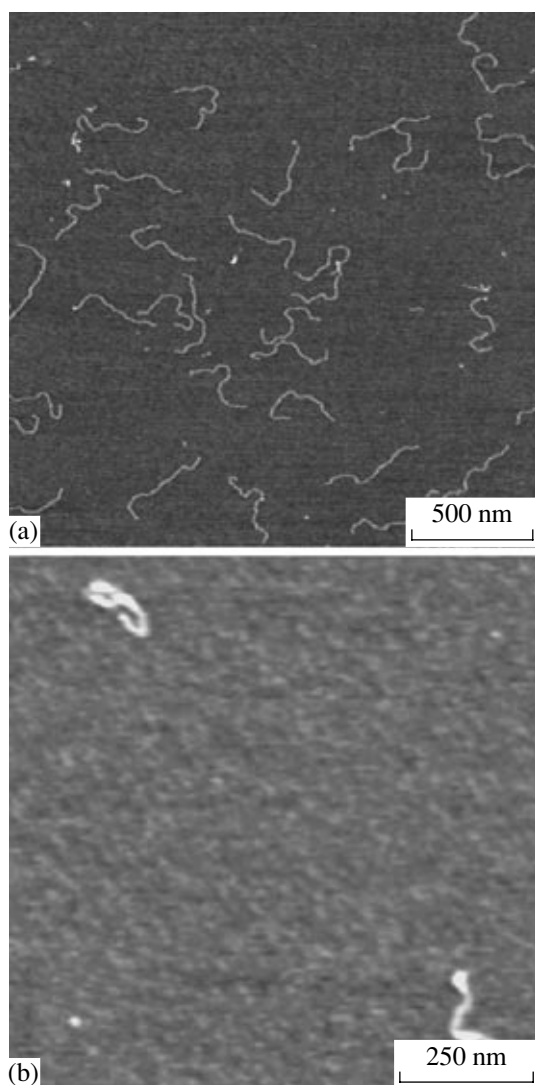


Fig. 8. AFM image of an amplified pGEMEX DNA fragment. (a) Freshly cleaved mica. The frame size is $2.2 \times 2.2 \mu\text{m}$. The expected contour length of the 1414-bp amplicon is $L = 480 \text{ nm}$ under the assumption that the DNA is a B-DNA ($H = 3.4 \text{ \AA}$). The contour length of the amplicon measured in the AFM image is $L = 435 \pm 15 \text{ nm}$, which corresponds to a rise per base pair along the double helix axis of $H = 3.07 \text{ \AA}$. (b) Modified amino mica with an increased surface charge density, i.e., an increased density of protonated amino groups. The frame size is $1 \times 1 \mu\text{m}$. The contour length of the amplicon is $L = 296 \pm 14 \text{ nm}$, which corresponds to a rise per base pair along the duplex axis of $H = 2.09 \text{ \AA}$.

What Is the Possible Mechanism of Oversupercoiling Supercoiled DNAs?

The structure of DNA molecules in solution, where they are negatively charged, is stabilized by van der Waals interactions, including the stacking interaction between neighboring nucleotide pairs, as well as the repulsion between neighboring phosphate groups of DNA. The change in the solution ionic strength alters the degree of shielding of the DNA phosphate groups

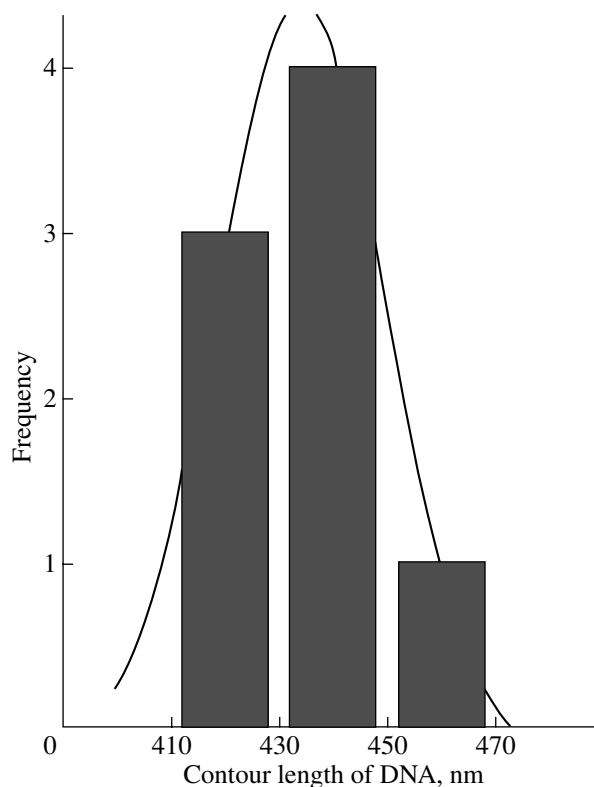


Fig. 9. Contour lengths of amplicons after PCR and subsequent purification measured in the AFM image of DNA immobilized on freshly cleaved mica. The curve shows the Gaussian distribution.

and, as a consequence, changes in the conformation of the molecule. In most studies on *in vitro* visualizing supercoiled DNAs by means of AFM, electron microscopy, and cryoelectron microscopy, the charges of DNA phosphate groups were neutralized in a comparatively narrow range by varying the ionic strength of the solution [11, 17, 25].

Although the degree of neutralizing of negatively charged phosphate groups of DNA is known to be the main factor of DNA supercoiling, the change in the ionic strength of the solution with the change in NaCl concentration or the change in the polycation concentration on the surface of mica used for immobilizing DNA were found [17–19] to cause only an insignificant DNA supercoiling (the supercoil density varied within the interval $0.03 < |\sigma| < 0.08$).

If pGEMEX DNA molecules were immobilized on the surface of freshly cleaved mica from a buffer solution containing Mg^{2+} ions, the AFM image showed plectonomic DNA molecules with a low supercoil density (Fig. 3a). Oversupercoiled or highly compact DNA were also not visualized in numerous experiments on model systems, including nucleosomes, aimed at determining the mechanism of DNA compaction with different proteins (histones, condensins, and cohesins) [26–29]. We think that the main reason

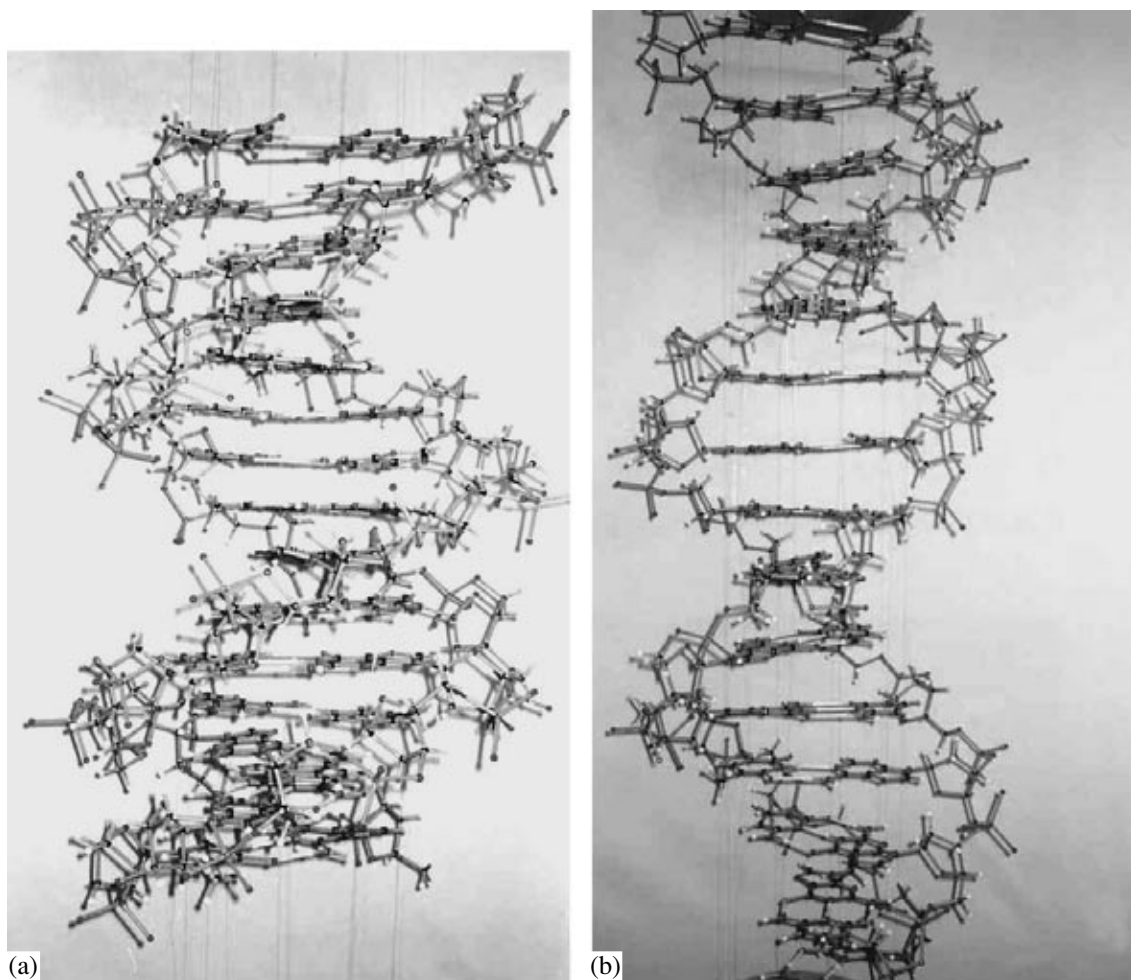


Fig. 10. The model of a 15-bp DNA fragment (a) in the S-form (the rise per base pair along the helix axis is $H = 2.0 \text{ \AA}$) and (b) in the B-form ($H = 3.4 \text{ \AA}$). The sequence of the + strand is 5'-aag gtc ttc ggt cgt-3'. The coil repeat for both DNA forms is 10.5 bp per coil.

for these negative results is that mica with a low surface charge density was used as an AFM substrate in most studies, with DNA being immobilized from a buffer solution containing Mg^{2+} ions. These ions, as well as Ca^{2+} ions, may interfere with the compaction of supercoiled DNA. For example, Ca^{2+} ions were demonstrated to interfere with the compaction of DNA in a complex containing the histone protein HMGB1.

Comparing supercoiled DNA visualized on standard amino mica (Fig. 2a) and on freshly cleaved mica, we can see that, in the first case, pGEMEX DNA molecules were more compact and less stretched, and single molecules occupied a smaller area. This may be explained by a stronger shielding of negatively charged DNA phosphate groups by the amino groups of mica and the resultant decrease in the electrostatic propulsion between neighboring DNA fragments. Several points should here be emphasized. In this study, we did not analyze the adhesive properties of the substrates used; suffice it to note that the surface

characteristics of mica can be estimated on the basis of the force curve (the dependence of the rupture force on the distance between the probe and the substrate) obtained by AFM in the force measurement mode. Earlier, we demonstrated that standard amino mica obtained by modifying in APTES vapor had a summary positive charge and an adhesion force of $F \sim 0.8\text{--}4.2 \text{ nN}$ in aqueous solutions at neutral pH [31]. However, we visualized only plectonomically supercoiled DNAs on standard amino mica. Only on modified amino mica, characterized by a higher charge surface density (according to our preliminary results, the amino group density on modified amino mica was two to three times higher than on standard amino mica), was it possible to visualize single oversupercoiled DNA molecules, even to the degree of formation of minitoroids and spheroids. In this case, biopolymer molecules with a high charge density (DNA) were placed on a substrate with a high charge surface density. Since the density of charged amino groups on the surface of modified amino mica was higher, a larger

number of negative phosphate groups of DNA was shielded. In addition, we assume that there is another, intramolecular, mechanism of DNA compaction, which may make a considerable contribution under the conditions of neutralizing the charge of phosphate groups. Theoretical calculations demonstrated that nucleotides along the DNA strand forming sites for ligand intercalation were differently charged. For example, the TA site is the most negative, because the 2'-deoxyribo-5'-monophosphate that is bound with adenine, the nitrous base with the highest positive charge, is the most negative. Therefore, the compaction of DNA may be accounted for by intramolecular electrostatic attraction between oppositely charged nucleotides under the conditions of an enhanced shielding of phosphate groups in DNA.

The results obtained indicate that oversupercoiling, leading to the compaction of single DNA molecules, may occur *in vitro* in the absence of proteins, however, it is necessary that the substrate surface on which the supercoiled DNA is immobilized should have a high surface positive charge density. This process results in both right and left oversupercoiled DNA molecules (Figs. 5 and 6, respectively). The results reported here suggest that supercoiled DNA immobilized on modified amino mica can be used to model transformations of natural DNA molecules *in vivo*, because the medium surrounding DNA in cell nuclei has a high density of positively charged residues of various molecules (mainly proteins).

ACKNOWLEDGMENTS

We are grateful to A. Sivolob of Kiev State University, A. Shestopalova of the Institute of Radio Electronics of the National Academy of Sciences of Ukraine, and O. Limanskaya of the Institute of Experimental and Clinical Veterinary Medicine for their fruitful discussion and constructive criticism of this paper. This study was supported by the International Center for Science and Technology, Japan, and by the Academy of Medical Sciences of Ukraine.

REFERENCES

- Ivanov V. 1983. DNA double helix. *Mol. Biol.* **17**, 616–621.
- Saenger W. 1984. *Principles of Nucleic Acid Structure*. N.Y.: Springer.
- Wang J. 1979. Helical repeat of DNA in solution. *Proc. Natl. Acad. Sci. USA.* **76**, 200–203.
- Cluzel P., Lebrun A., Heller C., Lavery R., Viovy J., Chatenay D., Caron F. 1996. DNA: An extensible molecule. *Science.* **271**, 792–794.
- Smith S., Cui Y., Bustamante C. 1996. Overstretching B-DNA: The elastic response of individual double-stranded and single-stranded DNA molecules. *Science.* **271**, 795–799.
- Leuba S., Karymov M., Tomschik M., Ramjit R., Smith P., Zlatanova J. 2003. Assembly of single chromatin fibers depends on the tension in the DNA molecule: Magnetic tweezers study. *Proc. Natl. Acad. Sci. USA.* **100**, 495–500.
- Bennink M., Leuba S., Leno G., Zlatanova J., De Grooth B., Greve J. 2001. Unfolding individual nucleosomes by stretching single chromatin fibers with optical tweezers. *Nature Struct. Biol.* **8**, 606–610.
- Rivetti C., Codeluppi S., Dieci G., Bustamante C. 2003. Visualizing RNA extrusion and DNA wrapping in transcription elongation complexes of bacteria and eukaryotic RNA polymerases. *J. Mol. Biol.* **326**, 1413–1426.
- Rivetti C., Codeluppi S. 2001. Accurate length determination of DNA molecules visualized by atomic force microscopy: Evidence for a partial B- to A-form transition on mica. *Ultramicroscopy.* **87**, 55–66.
- Lyubchenko Y., Gall A., Shlyakhtenko L., Harrington R., Jacobs B., Oden P., Lindsay S. 1992. Atomic force microscopy imaging of double stranded DNA and RNA. *J. Biomol. Struct. Dyn.* **10**, 589–606.
- Lyubchenko Y., Shlyakhtenko L. 1997. Visualization of supercoiled DNA with atomic force microscopy *in situ*. *Proc. Natl. Acad. Sci. USA.* **94**, 496–501.
- Shlyakhtenko L., Gall A., Filonov A., Cerovac Z., Lushnikov A., Lyubchenko Y. 2003. Silatrane-based surface chemistry for immobilization of DNA, protein–DNA complexes and other biological materials. *Ultramicroscopy.* **97**, 279–287.
- Limansky A. 2001. Analysis of aminomodified mica as a substrate for atomic force microscopy of nucleic acids. *Biopolim. Kletka.* **17**, 292–297.
- Limansky A., Shlyakhtenko L., Schaus S., Henderson E., Lyubchenko Y. 2002. Aminomodified probes for atomic force microscopy. *Probe Microsc.* **2**, 227–234.
- Butt H. 1991. Measuring electrostatic, van der Waals, and hydration forces in electrolyte solutions with an atomic force microscope. *Biophys. J.* **60**, 1438–1444.
- Hansma H., Golan R., Hsieh W., Daubendiek S., Kool E. 1999. Polymerase activities and RNA structures in the atomic force microscope. *J. Struct. Biol.* **127**, 240–247.
- Cherny D., Jovin T. 2001. Electron and scanning force microscopy studies of alterations in supercoiled DNA tertiary structure. *J. Mol. Biol.* **313**, 295–307.
- Tanigawa M., Okada T. 1998. Atomic force microscopy of supercoiled DNA structure on mica. *Anal. Chim. Acta.* **365**, 19–25.
- Bussiek M., Mucke N., Langowski J. 2003. Polylysine-coated mica can be used to observe systematic changes in the supercoiled DNA conformation by scanning force microscopy in solution. *Nucleic Acids Res.* **31**, 1–10.
- Limansky A. 2002. Analysis of aminomodified probes for atomic force microscopy of biological molecules. *Biopolim. Kletka.* **18**, 62–70.
- Limansky A., Limanskaya O. 2002. Analysis of genomic DNA by atomic force microscopy. *Tsitol. Genet.* **36** 30–6.
- Mazur G., Jernigan R., Sarai A. 2003. Conformational effects upon DNA stretching. *Mol. Biol.* **37**, 277–287.
- Shlyakhtenko L., Gall A., Weimer J., Hawn D., Lyubchenko Y. 1999. Atomic force microscopy imaging of

- DNA covalently immobilized on a functionalized mica substrate. *Biophys. J.* **77**, 568–576.
24. Vologodsky A. 1988. *Topologiya i fizicheskie svoystva kol'tsevykh DNK* (Topology and Properties of Circular DNAs). Moscow: Nauka.
 25. Boles T., White, Cozzarelli N. 1990. Structure of plectonometrically supercoiled DNA. *J. Mol. Biol.* **213**, 931–951.
 26. Conwell C., Vilfan I., Hud N. 2003. Controlling the size of nanoscale toroidal DNA condensates with static curvature and ionic strength. *Proc. Natl. Acad. Sci. USA.* **100**, 9296–9301.
 27. Kemura K., Rybenkov V., Crisona N., Hirano T., Cozzarelli N. 1999. 13S Condensin actively reconfigures DNA by introducing global positive writhe: Implications for chromosome condensation. *Cell.* **98**, 239–248.
 28. Hizume K., Yoshimura S., Maruyama H., Kim J., Wada H., Takeyasu K. 2002. Chromatin reconstitution: Development of a salt-dialysis method monitored by nanotechnology. *Arch. Histol. Cytol.* **65**, 405–413.
 29. Yoshimura S., Hizume K., Murakami A., Sutani T., Takeyasu K., Yanagida M. 2002. Condensin architecture and interaction with DNA: Regulatory non-SMC subunits bind to the head of SMC heterodimer. *Curr. Biol.* **12**, 508–513.
 30. Polyanchko A.M., Chikhirzhina E.V., Andrushchenko V.V., Kostyleva E.I., Wieser H., Vorob'ev V.I. 2004. The effect of Ca²⁺ ions on DNA compaction in the complex with nonhistone chromosomal HMG1 protein. *Mol. Biol.* **38**, 701–712.
 31. Limansky A. 2003. Atomic force microscopy: From visualizing DNA and protein molecules to measuring the force of intermolecular interactions. *Usp. Sovrem. Biol.* **123**, 531–542.
 32. Newlin D., Miller K., Pilch D. 1984. Interactions of molecules with nucleic acids: 7. Intercalation and T–A specificity of daunomycin in DNA. *Biopolymers.* **23**, 139–158.